

# Capping Strategies for Covalent Template-Directed Synthesis of Linear Oligomers using CuAAC

Maria Ciaccia, Diego Núñez-Villanueva and Christopher A. Hunter.\*

Department of Chemistry, University of Cambridge, Lensfield Road, Cambridge CB2 1EW, UK.

*Copper catalyzed azide alkyne cycloaddition, template-directed synthesis, covalent base-pair, oligomer, effective molarity*

---

**ABSTRACT:** Covalent templating provides an attractive solution to the controlled synthesis of linear oligomers, because a template oligomer can be used to define the precise length and sequence of the product. If the monomer units are attached to the template using kinetically inert covalent bonds, it should be possible to operate at high dilution to favour intramolecular over intermolecular reaction. However, for oligomerisation reactions using copper catalysed azide alkyne cycloaddition (CuAAC) this is not the case. The rate limiting step is formation of an activated copper complex, so any alkyne that is activated by copper reacts rapidly with the nearest available azide. As a result, every time a chain end alkyne is activated, rapid intermolecular reaction takes place with a different oligomer leading to the formation of higher order products. It proved possible to block these intermolecular reactions by adding an excess of an azide capping agent that intercepts the chain end of the growing oligomer on the template. By adjusting the concentration of the capping agent to compete effectively with the unwanted intermolecular reactions without interfering with the desired intramolecular reactions, it was possible to obtain quantitative yields of copy strands from covalent template-directed oligomerisation reactions. Remarkably the capping agent could also be used to control the stereochemistry of the duplex formed in the templated oligomerisation reaction to give exclusively the antiparallel product.

---

## INTRODUCTION

Template-directed synthesis is a powerful tool for the construction of complex molecular architectures.<sup>1-9</sup> Conventionally, templating is used to direct ring closure of a macrocyclic product, as first described for crown ether synthesis half a century ago.<sup>4,8-12</sup> Macrocyclic oligomers are attractive targets, because after ring closure takes place no further reaction is possible. Linear oligomers represent a more challenging synthetic target, because the chain ends carry reactive groups that can undergo further reaction.<sup>13</sup>

Non-covalent templating has become the method of choice for macrocycle synthesis, because removal of the template after the reaction has taken place is usually straightforward. However, covalent template-directed synthesis<sup>14-22</sup> offers a number of advantages over the non-covalent approach. When the building blocks are attached to the template using kinetically inert covalent bonds, it is possible to isolate and characterise the key intermediates, which are difficult to identify in systems where all species are in dynamic equilibrium. In covalent templating, separate steps are used for attachment of reactants to the template and the templated reaction. Quantitative attachment to the template can be driven by using very high concentrations of reactants, and intramolecular reactions on the template can be favoured over competing intermolecular reactions by using very low concentrations in the templated reaction step. These options are not available in non-covalent systems, where attachment of reactants to the template and the templated reaction take place in the same step. In non-covalent template-directed synthesis, the choice of concentration is compromised: high concentrations are required to ensure efficient binding of reactants to the template and low concentrations are required to ensure intramolecular reactions on the template are faster than competing intermolecular

reactions.<sup>23</sup> The products from covalent templating are kinetically stable compounds, and so the origin of any side-products in the templated reaction can be investigated by characterising the structures of the template-bound species, providing an opportunity for rational reaction optimisation. Covalent template-directed synthesis is therefore particularly well-suited to templating the construction of challenging targets such as linear oligomers.

Template-directed synthesis of linear oligomers is one of the most important processes in biology. Synthesis of DNA, RNA and proteins all rely on the transfer of sequence information from a nucleic acid template to a templated product.<sup>24-26</sup> These processes are all controlled by complex enzymatic machinery that adds monomer units stepwise onto a growing chain end. Start and stop sites for linear oligomer synthesis are programmed into the nucleic acid template, so the chain ends of the templated product are well-defined, and the error rates are extremely low.

One of the challenges in template-directed synthesis of linear oligomers is that the reactive chain ends can lead to uncontrolled polymerization, unless start and stop sites are built into the templating process. Control can be achieved through concentration, reaction time or addition of end-capping reagents to minimize undesired reactions at chain ends.<sup>13</sup> We have been working on the development of a chemical approach to the template-directed synthesis of linear oligomers that uses kinetically inert covalent base-pairing as the basis for sequence information transfer between parent and daughter strands.<sup>27</sup> Realisation of an efficient process would open the way for the application of molecular evolution to search the huge chemical space constituted by synthetic mixed sequence oligomers.<sup>28,29</sup> The *in situ* capping reactions described in this paper represent an important step in that direction.

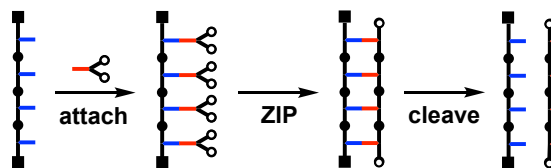


**Figure 1.** Covalent template-directed synthesis of a linear oligomer. In the *attach* step, monomers (red) are coupled with complementary groups on the template (blue). In the *ZIP* step, intramolecular reactions between complementary reaction sites on the monomers (white dots) lead to oligomerisation. In the *cleave* step, the bonds connecting the new oligomer to the template are broken to regenerate the template (blue) and release the product (red).

Figure 1 shows the key steps in the covalent template-directed synthesis of a linear oligomer. The monomer units are equipped with a functional group (red) that can be used for pairing with complementary sites on the template (blue) and two reactive groups (white dots) that can be coupled to give linear oligomers. In the first step, the monomer units are attached to the template strand by formation of covalent base-pairs. In the *ZIP* step, oligomerisation of the

monomer units takes place on the template. Finally, the covalent base-pairs are cleaved to regenerate the template and release the complementary copy.

Figure 2 shows how this approach was used for covalent template-directed synthesis of a mixed sequence linear trimer.<sup>27</sup> The base-pairing chemistry used to attach the monomers to the template is formation of esters between phenols and benzoic acids. Selective protection and deprotection of the phenol group on the template allowed sequential attachment of the phenol monomers to the benzoic acids on the template followed by attachment of the benzoic acid monomer to the phenol on the template to give the pre-*ZIP* intermediate shown in Figure 2. The backbone chemistry used in the *ZIP* step is the CuAAC reaction<sup>30-32</sup> between the alkyne and azide groups on the monomers, which resulted in an oligotriazole backbone in the product duplex. Hydrolysis of the esters cleaved the base-pairs to regenerate the template and release the product strand. One end of the product strand was capped *in situ* with an azide in the *ZIP* step, and the other end was capped with an alkyne after the cleave step to give the sequence-complementary copy of the template.

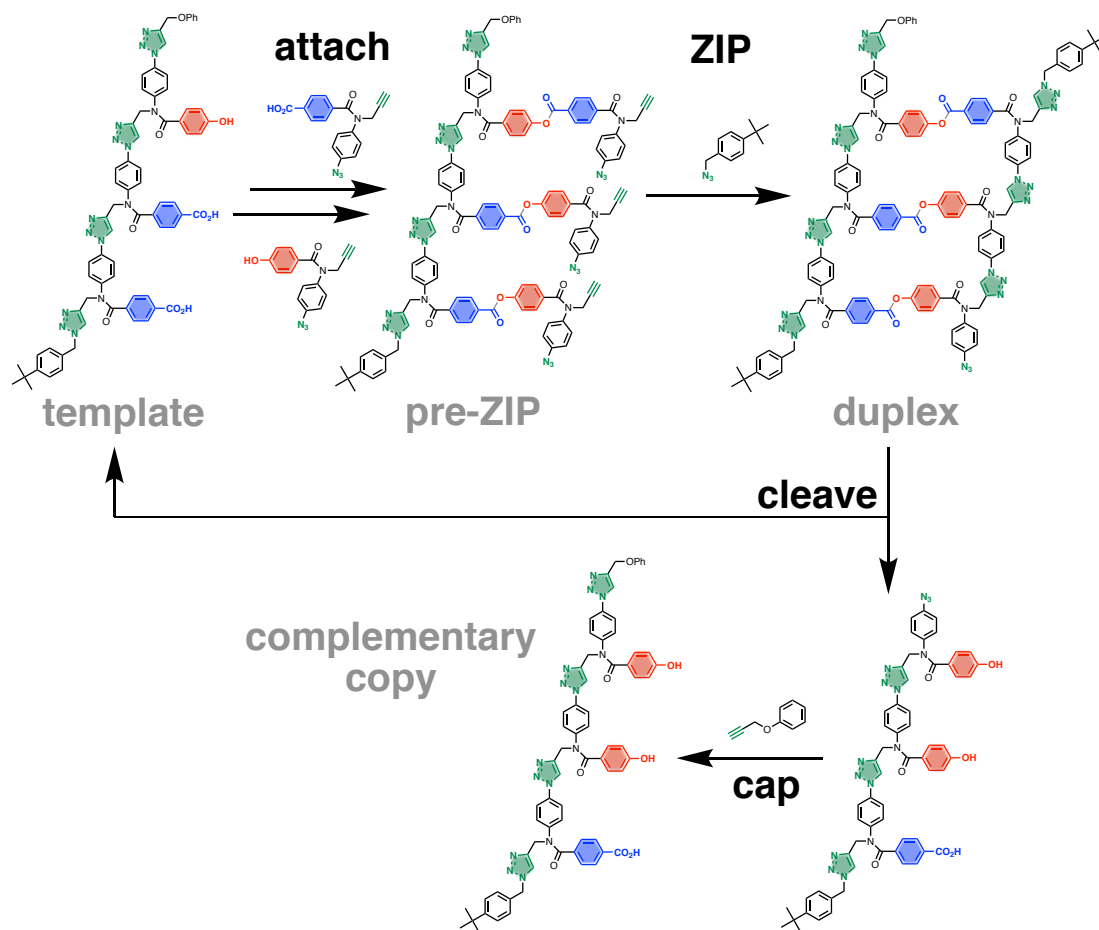


**Figure 2.** Covalent template-directed synthesis of a mixed sequence linear trimer using ester base-pairs and CuAAC coupling reactions in the *ZIP* step. A series of protection-coupling-deprotection-coupling reactions was used to attach the monomer units to the template. The *ZIP* step was carried out in the presence of an azide to cap one chain end, and a second cap was added to the other chain end after cleavage from the template.<sup>27</sup>

All of the steps in the covalent template-directed synthesis pathway shown in Figure 2 proceeded in remarkably high yield, but the presence of the capping azide in the *ZIP* step proved to be crucial to success. Figure 3 illustrates why the *ZIP* step is likely to be the most

difficult part of the templating cycle. A large number of different intermolecular and intramolecular reactions are possible. By operating at low concentrations, it should be possible to favour the intramolecular reaction channel over the competing intermolecular reaction

channels. However, even if the intramolecular channel is highly favoured, the templated product duplex still carries two reactive functional groups on the chain ends. The yield of the templated product is likely to be degraded by slow intermolecular oligomerisation processes or by intramolecular cyclisation of the chain ends to give macrocycles. End-capping strategies are widely used in polymer synthesis for chain-length control and chain-end functionalization.<sup>33-37</sup> Here we investigate the role of capping agents in controlling the product distribution of template-directed synthesis of linear oligomers and show that the choice of reagent as well as the concentration regime is critical to the outcome. The experiments also provide fundamental insight into the mechanistic aspects of the CuAAC reaction.

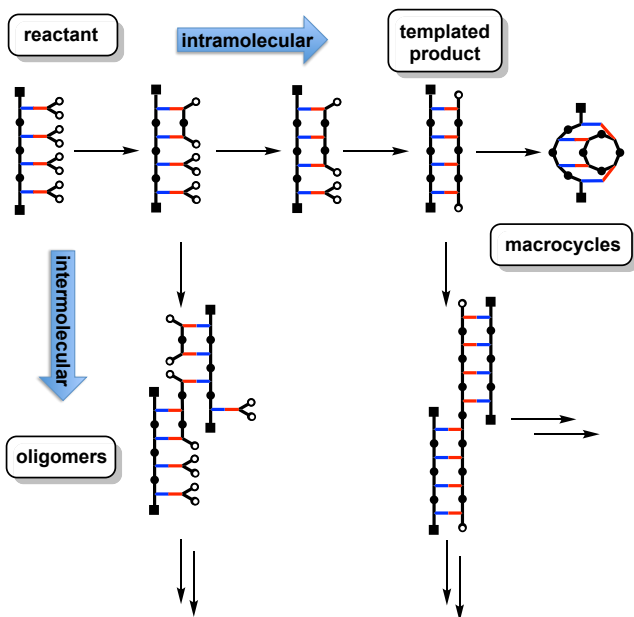


**Figure 3.** Competing reaction pathways in the template synthesis of a linear oligomer. The intramolecular channel leads to the desired *templated product*, and the competing intermolecular reaction channels lead to higher order *oligomers*. The two terminal reactive sites in the *templated product* (white dots) can react further through intramolecular reactions to give *macrocycles*.

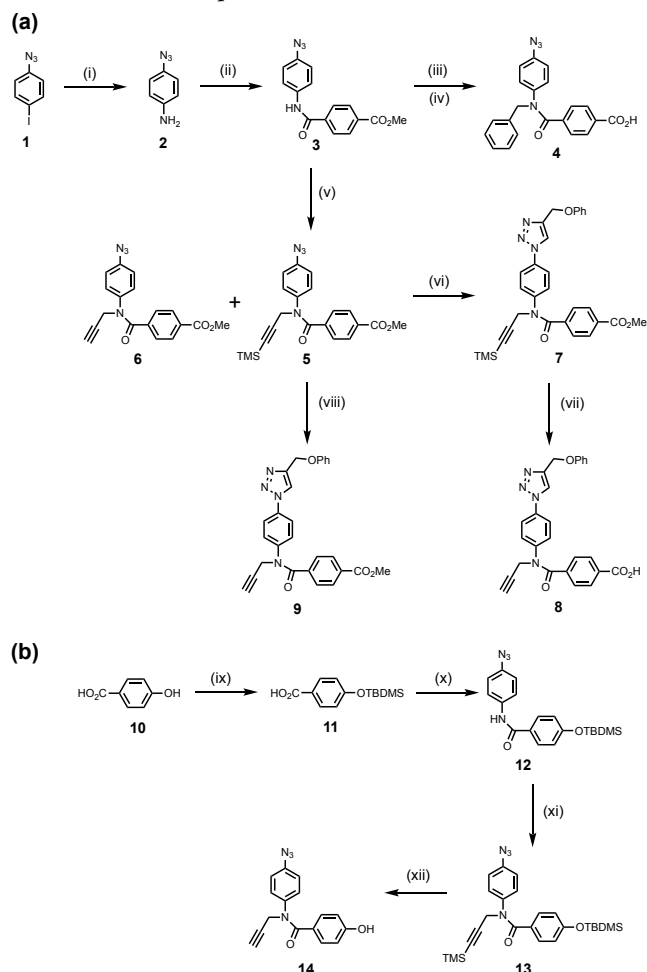
## RESULTS AND DISCUSSION

The CuAAC ZIP reaction was investigated using two different dimer templates: a homo-dimer and a hetero-dimer. Monomer units equipped with reactive functional groups were attached to the templates, and the products formed in the presence and absence of a capping agent were characterised. The product of the ZIP reaction on a dimer template is a linear dimer, which cannot react further to give the cyclic dimer due to ring strain, so this system provides an opportunity to investigate how capping agents can be used to intercept intermolecular oligomerisation reactions without competition from intramolecular macrocyclisation. The hetero-dimer template allows attachment of two different monomer units, and this system was used to investigate the subtleties of the reaction kinetics that determine the optimum choice of capping agent and conditions.

### Synthesis

Synthesis of the benzoic acid and phenol monomer building blocks is shown in Scheme 1. *p*-Azidoaniline **2** was synthesised from **1** using literature procedures<sup>38</sup> and coupled with mono-methyl

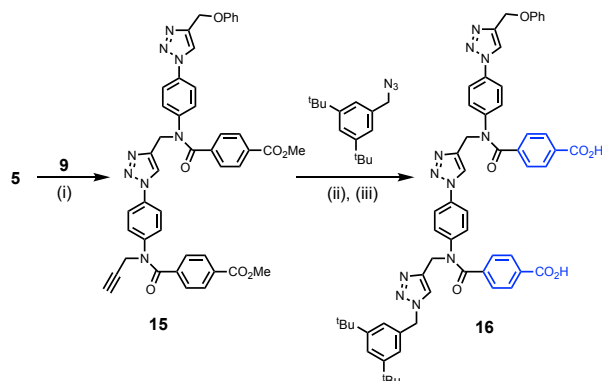
terephthalate using EDC to give **3** (Scheme 1(a)).<sup>27</sup> Amide **3** was alkylated with sodium hydride and benzyl bromide, and subsequent hydrolysis of the ester moiety with lithium hydroxide gave the mono-capped benzoic acid monomer **4**. Alkylation of **3** with sodium hydride and TMS protected propargyl bromide afforded compound **5** and a small percentage of deprotected ester **6**. CuAAC reaction of **5** with phenyl propargyl ether using copper(I) tetrakis(acetonitrile) hexafluorophosphate and tris[(1-benzyl-1*H*-1,2,3-triazol-4-yl)methyl]amine (CuTBTA) gave **7**. Reaction of **7** with lithium hydroxide afforded the mono-capped benzoic acid monomer **8**. Deprotection of **7** with TBAF gave ester **9**. The protected phenol monomer **13** was synthesised from 4-hydroxybenzoic acid **10** (Scheme 1(b)) by protecting the phenol with TBDMS-Cl, followed by EDC coupling with aniline **2**, and then alkylation with sodium hydride and TMS protected propargyl bromide. Deprotection of both phenol and alkyne with TBAF afforded the phenol monomer **14**.



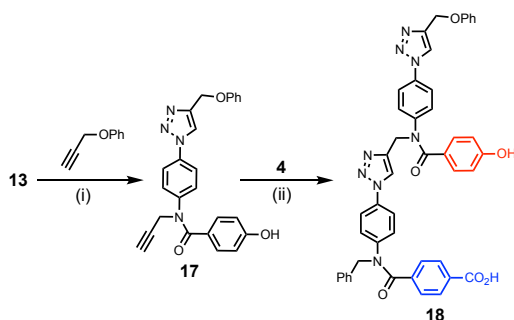
**Scheme 1.** Synthesis of benzoic acid (a) and phenol (b) building blocks: (i) NaN<sub>3</sub> (96%); (ii) EDC, DMAP (98%); (iii) benzyl bromide, NaH; (iv) LiOH (44% over two steps), (v) TMS-propargyl bromide, NaH (81%); (vi) phenyl propargyl ether, Cu(CH<sub>3</sub>CN)<sub>4</sub>PF<sub>6</sub>, TBTA (73%); (vii) LiOH (95%); (viii) TBAF (81% from **5**); (ix) TBDMS-Cl, imidazole (92%); (x) EDC, DMAP (97%); (xi) TMS-propargyl bromide, NaH (72%); (xii) TBAF (quant.).

Scheme 2 shows the synthesis of the homo-dimer template **16**. The protected benzoic acid monomer, **5**, and the capped benzoic acid monomer **9** were coupled using a CuAAC reaction, followed by

TBAF deprotection, to give **15**. Another CuAAC reaction with 1-(azidomethyl)-3,5-di-*t*-butylbenzene, followed by ester hydrolysis with LiOH, afforded template **16**. Scheme 3 shows the synthesis of the hetero-dimer template **18**. The protected phenol monomer, **13**, and phenyl propargyl ether were coupled using a CuAAC reaction, followed by TBAF deprotection, to give **17**. A second CuAAC reaction with the capped benzoic acid monomer **4** gave template **18**.



**Scheme 2. Synthesis of template 16:** (i)  $\text{Cu}(\text{CH}_3\text{CN})_4\text{PF}_6$ , TBTA, then 1 M TBAF (93%); (ii)  $\text{Cu}(\text{CH}_3\text{CN})_4\text{PF}_6$ , TBTA (76%); (iii) LiOH (67%).



**Scheme 3. Synthesis of template 18:** (i)  $\text{Cu}(\text{CH}_3\text{CN})_4\text{PF}_6$ , TBTA, then 1 M TBAF (70%); (ii)  $\text{Cu}(\text{CH}_3\text{CN})_4\text{PF}_6$ , TBTA (86%).

#### Untemplated Oligomerisation of Monomers

The behaviour of the monomer units in the absence of template was first investigated. This experiment provides a useful measure of the propensity of linear oligomers to form macrocycles in the absence of any capping agent. Figure 4(a) illustrates the oligomerisation process for a monomer bearing an alkyne and an azide and the products that can be formed in a CuAAC reaction. Figure 4(b) shows the HPLC chromatogram of the crude product mixture obtained when monomer **6** was oligomerised using CuTBTA. The two major peaks correspond to species that have molecular weights three and four times that of the starting material. The IR spectra of these compounds showed that in both cases the azide stretch that was observed at  $2100\text{--}2200\text{ cm}^{-1}$  in the starting material was not present. The two major products of the oligomerisation reaction are therefore the cyclic trimer and cyclic tetramer. No cyclic dimer was detected, presumably due to the excessive ring strain. Thus dimer templates will allow us to explore the competition between intermolecular and intramolecular reactions with no competition from intramolecular macrocyclisation processes.

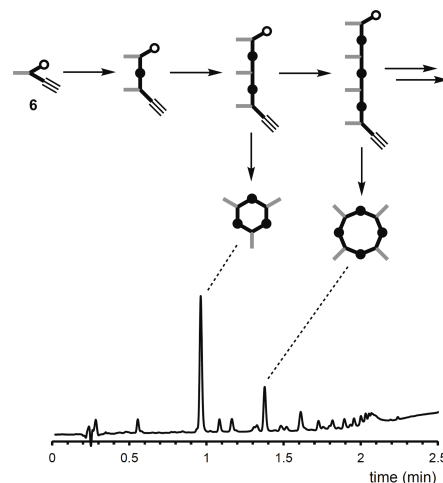
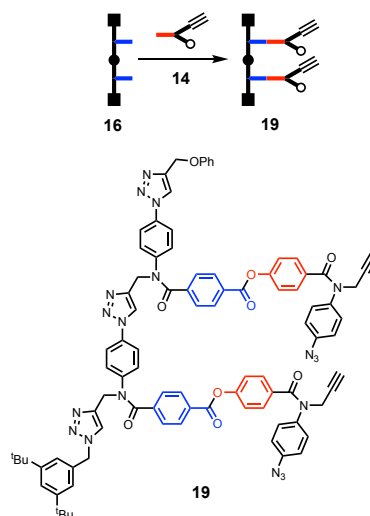


**Figure 4.** HPLC chromatogram for the CuAAC oligomerisation of **6** ( $50\ \mu\text{M}$ ) and CuTBTA ( $500\ \mu\text{M}$ ) in THF at room temperature. A cartoon representation of the reaction pathway is shown, and the structures corresponding to the two major products are indicated.

#### ZIP Reactions on the Homo-Dimer Template

The phenol monomer **14** was loaded onto the homo-dimer template **16** using EDC coupling to give pre-ZIP intermediate **19** (Scheme 4).



**Scheme 4.** Attachment of monomers to homo-dimer template **16** to give pre-ZIP intermediate **19** (EDC, DMAP, 65%).

Figure 5 shows the result of subjecting this compound to a CuAAC reaction. The crude reaction mixture was analysed as a function of time using LCMS, and a number of different products were observed. The two major product peaks observed in the HPLC chromatograms in Figure 5(a) are labelled 1 and 2, and Figures 5(b) and 5(c) show the corresponding mass spectra. Peak 1 has the same molecular weight as the starting material but a different retention time, which suggests that it is the product of the intramolecular ZIP reaction. Peak 2 has double the molecular weight of the starting material, which indicates that this product is due to an intermolecular reaction. The smaller peaks, labelled 3 and 4 in Figure 5(a), also have double the molecular weight of the starting material (Figure 5(d)). Peaks 3 and 4 appear and then disappear, whereas the product corresponding to peak 2 accumulates and is the major species detected at long reaction times. Another small peak, labelled 5 in Figure 5(a),

was detected at long reaction times. The corresponding mass spectrum shown in Figure 5(d) shows that this product has a molecular weight that is three times the molecular weight of the starting material.

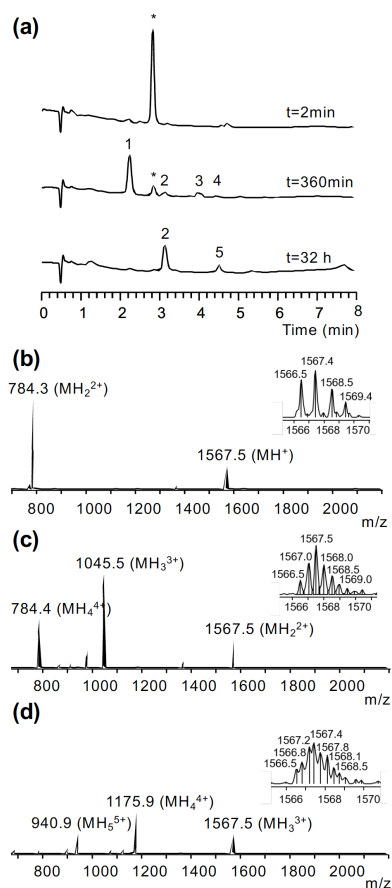


**Figure 5.** (a) HPLC chromatograms recorded at different time points (t) in the CuAAC reaction of **19** (50  $\mu$ M) and CuTBTA (50  $\mu$ M) in THF at room temperature. The starting material **19** is labelled with an asterisk, and other peaks are numbered. (b) Mass spectrum of peak 1. (c) Mass spectrum of peak 2. (d) Mass spectrum of peak 5. The isotope patterns shown for the peaks labelled 1567.5 were used to assign these species as the +1, +2 and +3 ion in (b), (c) and (d) respectively.

Figure 6(a) illustrates different intramolecular and intermolecular reaction pathways that are possible in this system. Based on the mass spectrum shown in Figure 5(b), peak 1 in the HPLC chromatogram can be assigned as **20**, which is formed when the intramolecular ZIP reaction takes place on the template to give the desired linear dimer. However, this species is rapidly consumed, and peak 2 is the major product at longer reaction times. Based on the fact that peak 2 accumulates, whereas peaks 3 and 4 are intermediates, peak 2 is tentatively assigned as **22**, the macrocyclic tetramer formed by an intermolecular reaction followed by cyclisation. Peaks 3 and 4 are assigned as intermediates (for example **21** shown in Figure 6(a)) that are formed by intermolecular reactions involving different combinations of **19** and **20**. By analogy with peak 2, peak 5 in the final HPLC chromatogram in Figure 5(a) is tentatively assigned as the macrocyclic hexamer formed due to further intermolecular reaction of intermediates such as **21** followed by cyclisation.

Figure 6(b) shows the evolution of the product distribution as a function of reaction time. The intramolecular ZIP reaction to form

the linear dimer **20** is rapid (red data), but this product is quickly consumed, because the intermolecular reaction to give **21** (dark blue) is also rapid. Finally, a slower intramolecular reaction converts **21** to the cyclic tetramer **22** (pale blue), which is the major product after several hours. There is no time point at which the template-directed ZIP reaction to give **20** is complete with no side-products due to intermolecular reactions. In principle, the relative rates of the intermolecular and intramolecular reactions can be controlled using concentration. The ZIP reaction was therefore repeated at a 2-fold lower concentration of **19** in the hope of suppressing the undesired intermolecular processes. The evolution of the product distribution as a function of reaction time under these conditions is illustrated in Figure 6(c). Surprisingly, the result is practically identical to that obtained at the higher concentration (Figure 6(b)). The origin of this phenomenon will be discussed in more detail below in relation to the mechanism of the CuAAC reaction. However, these observations indicate that it will not be possible to control the product distribution using concentration and that a different strategy is required to suppress the undesired intermolecular reaction pathways.

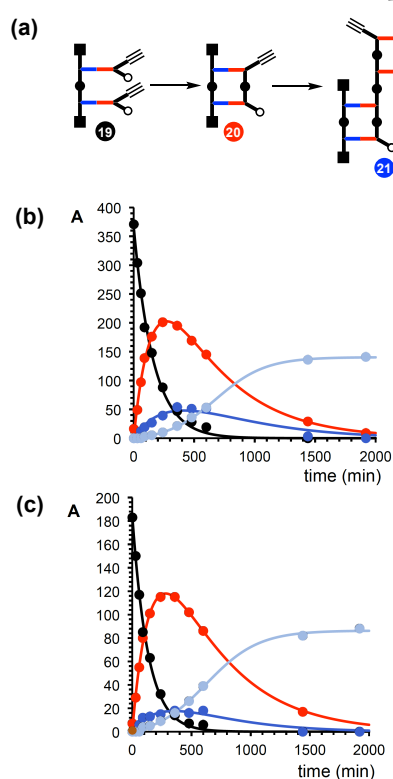


**Figure 6.** (a) Cartoon representation of the CuAAC reaction of **19**. (b) Time dependence of the product distribution plotted as HPLC peak area (A) for the reaction of **19** (50  $\mu$ M) and CuTBTA (50  $\mu$ M) in THF at room temperature. (c) Time dependence of the product distribution for the reaction of **19** (25  $\mu$ M) and CuTBTA (50  $\mu$ M) in THF at room temperature. The lines are drawn as a guide (black **19**, red **20**, dark blue is the sum of the peak areas of all **21**-like intermediates, pale blue is the sum of the areas of peaks 2 and 5, i.e. intermolecular products like **22**).

#### Effect of a Capping Agent on ZIP Reactions on the Homo-Dimer Template

The effect of adding 4-*t*-butylbenzyl azide to the reaction mixture was then investigated. This compound should act as a capping agent by intercepting the unreacted alkyne on the linear dimer **20** and so block all subsequent intermolecular reactions. Figure 7(a) shows the

three different products that were identified in the crude reaction mixture by LCMS. The amount of tetramer formed due to intermolecular reactions was negligible, and after 24 hours, the only major product was the capped linear dimer **24**. Figure 7(b) shows the evolution of the product distribution as a function of reaction time. Interestingly, the intramolecular ZIP reaction to form **20** (red) and the intermolecular reaction with the capping azide to form the acyclic intermediate **23** (grey) occur at similar rates. However, both of these products are converted to **24** (orange), which has no free alkyne groups for further reaction. No doubly capped product **25** was observed under these conditions. Thus, the capping agent provides an effective method for preventing the intermolecular side reactions observed in the ZIP step of the template-directed synthesis of the phenol homo-dimer.

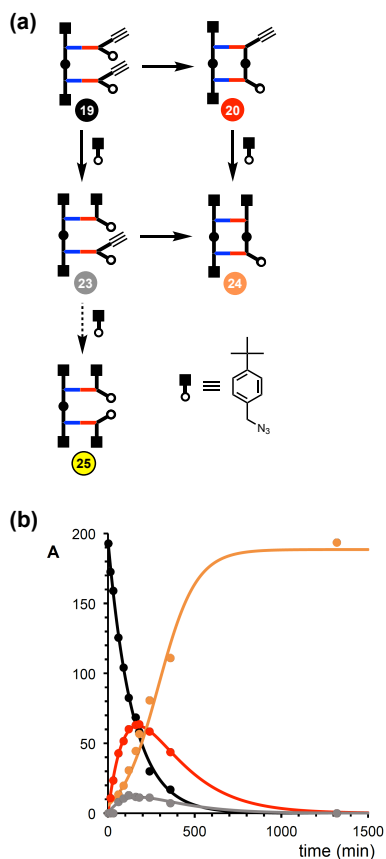


**Figure 7.** (a) Cartoon representation of the CuAAC reaction of **19** in the presence of a capping agent. (b) Time dependence of the product distribution plotted as HPLC peak area (A) for the reaction of **19** (25  $\mu$ M), CuTBTA (50  $\mu$ M) and 4-*t*-butylbenzyl azide (1.25 mM) in THF at room temperature. The lines are drawn as a guide (black **19**, red **20**, grey **23**, orange **24**).

The product of the ZIP reaction of **19** in the presence of the capping agent was characterised by  $^1\text{H}$  NMR spectroscopy (Figure 8). A total of 10 different triazole signals were observed, but **24** only contains 5 non-equivalent triazole rings. Variable temperature experiments show that the doubling of the number of triazole signals is unlikely to be due to the interconversion of two different conformers in slow exchange on the  $^1\text{H}$  NMR timescale. The signals move and sharpen with temperature, suggesting that there is some conformational rearrangement, but the relative intensities are unaffected (Figure 8). The doubling of the number of signals in the  $^1\text{H}$  NMR spectrum is more likely due to the presence of two isomeric products.

The product of the ZIP reaction is a duplex, and the backbones have a direction, so parallel and antiparallel arrangements are possible (Figure 9). Integration of the triazole signals indicates that there are two different species present in a ratio of 2:1 (labelled green and purple in Figure 8). The experiments described in the following section were used to assign the green and purple  $^1\text{H}$  NMR signals as the antiparallel and parallel duplexes respectively.

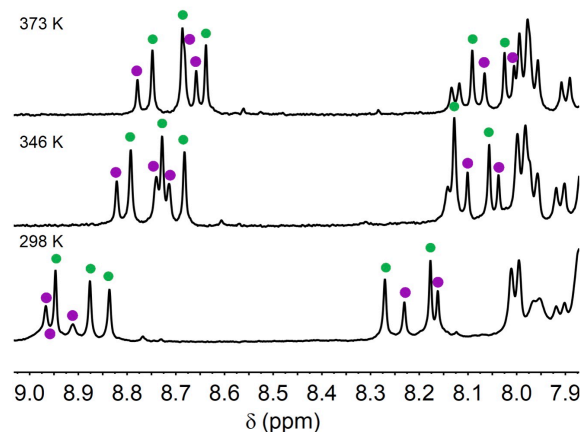


**Figure 8.** Triazole region of 500 MHz  $^1\text{H}$  NMR spectra of the product obtained from the CuAAC reaction of **19** (25  $\mu$ M), CuTBTA (50  $\mu$ M) and 4-*t*-butylbenzyl azide (1.25 mM) in THF at room temperature. Spectra were recorded in  $\text{DMSO-}d_6$  at different temperatures. Signals due to the antiparallel (**a-24**) and parallel (**p-24**) duplexes are labelled with green and purple dots respectively.

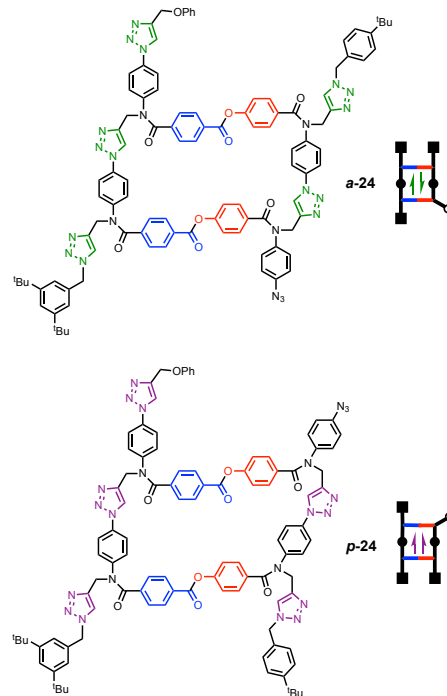


**Figure 9.** Structures of the antiparallel (**a-24**) and parallel (**p-24**) duplexes formed in the CuAAC reaction of **19**.

The rate of the intermolecular reaction with the capping agent should depend on the concentrations used. In contrast, the rate of the intramolecular ZIP reaction is expected to be concentration independent and to depend only on the effective molarity (EM) of the two reacting groups present in the pre-ZIP intermediate **19**.<sup>39</sup> Figure

10 shows the result of varying the concentration of the capping agent on the product distribution. The proportion of intermolecular reaction leading to oligomerisation (blue data) drops with increasing concentrations of capping agent. At higher concentrations of capping agent, intermolecular reaction with the capping agent begins to compete with the intramolecular ZIP reaction leading to the doubly capped product **25**, which is shown in Figure 7(a) (yellow data in Figure 10). The sweet spot under these reaction conditions occurs when the concentration of capping agent is 2.5 mM, which leads to a very efficient process giving **24** as the only significant product (orange data in Figure 10).

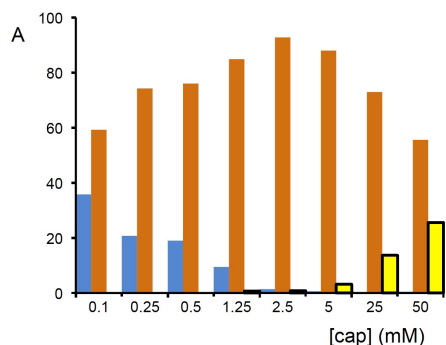


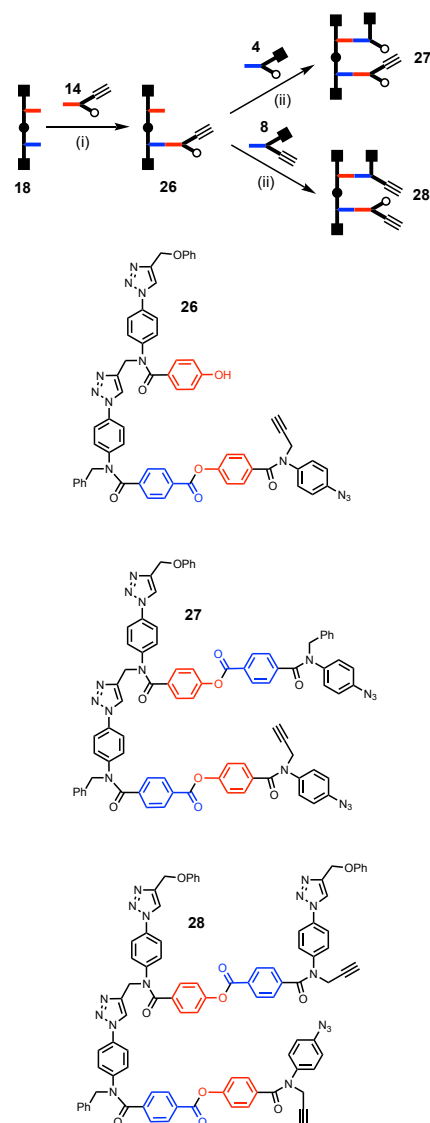
**Figure 10.** Product distribution of the CuAAC reaction of **19** in the presence of different concentrations of capping agent (4-*t*-butylbenzyl azide). The areas of the HPLC peaks assigned to **24** (orange) and **25** (yellow) and the sum of the areas of the peaks assigned to oligomeric products (blue) are plotted as a percentage of the total of all peak areas (A). Reactions were carried out using **19** (25  $\mu$ M) and CuTBTA (50–500  $\mu$ M) in THF at room temperature.

#### ZIP reactions on the hetero-dimer template

Figure 10 shows that very high concentrations of capping agent lead to competition with the desired ZIP reaction, because the alkyne required for the intramolecular reaction reacts intermolecularly with the capping agent. These two competing reaction pathways provide a convenient method for measuring EM values for the intramolecular processes. The EM for the intramolecular process can be determined from the concentration of capping azide at which the yield of the duplex from the intramolecular reaction is the same as the yield of the doubly capped product from the intermolecular reaction. This experiment also provides a convenient method to investigate the difference between the values of EM for the parallel and antiparallel ZIP reactions. However, more complex pre-ZIP intermediates are required, where the directionality of the backbone can be specified by the structures of the starting materials. The hetero-dimer template provided us with a route to suitable compounds (Scheme 5).

In order to independently measure values of EM for the parallel and antiparallel ZIP reactions, a mixed sequence template, **18**, and mono-capped monomers, **14** and **4**, were used (Scheme 5). The phenol moiety on template **18** was selectively protected with TBDMS. The benzoic acid moiety on the template could then be coupled with phenol monomer **14** using EDC. Deprotection of the phenol moiety on the template with TBAF gave **26**. EDC coupling of **26** with a benzoic acid monomer, which lacks the reactive alkyne group, **4**, gave pre-ZIP intermediate **27**, which can only form an antiparallel duplex in an intramolecular CuAAC reaction. Similarly, EDC coupling of **26** with a benzoic acid monomer, which lacks the

reactive azide group, **8**, gave pre-ZIP intermediate **28**, which can only form a parallel duplex in an intramolecular CuAAC reaction.



**Scheme 5.** Attachment of monomers to template **18** to give mono-capped pre-ZIP intermediates **27** (71%) and **28** (61%): (i) 1. TBDMS-Cl, imidazole; 2. **14**, EDC, DMAP; 3. TBAF. (ii) EDC, DMAP.

CuAAC reactions were carried out on **27** and **28** in the presence of different concentrations of the capping azide, and the product distribution was determined by LCMS. In both cases, two different products were identified: the duplex formed by intramolecular reaction (**29** or **34**) and the acyclic product due to intermolecular reaction with the capping agent (**30** or **35**). The reaction pathways leading to these products are shown in Figure 11. In **27**, there is only one alkyne, which can either react in intramolecular fashion to form the antiparallel duplex **29** or it can react with the capping azide to form the acyclic species **30** (Figure 11(a)). In **28**, there are two reactive alkynes, so there are multiple reaction pathways, but they converge to only two products (Figure 11(b)). One of the alkynes can either react in an intramolecular fashion to form the parallel duplex **31** or it can react with the capping azide to form the acyclic species **32**. The other alkyne can only react with the capping azide in an intermolecular fashion giving the two final products, **34** and **35**.

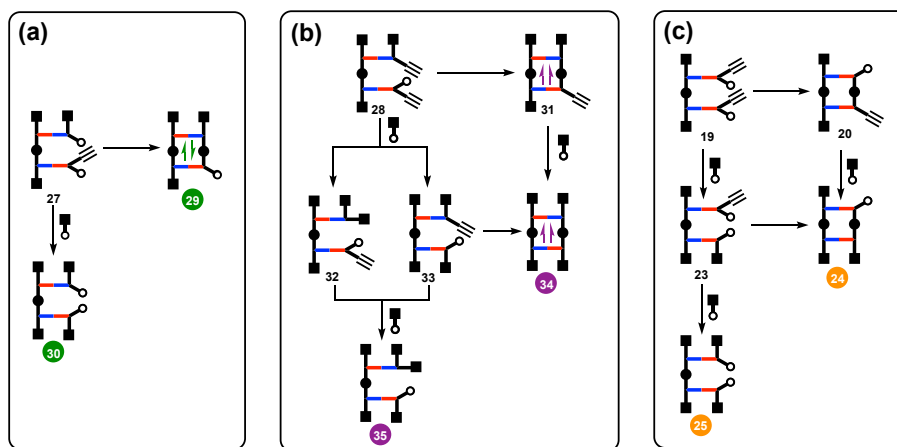


**Figure 11.** Cartoon representation of reaction pathways in the CuAAC reaction of **27** (a), **28** (b) and **19** (c) in the presence of a capping agent. The orientation of backbones in the product duplexes is indicated with arrows where known.

The ratio of intramolecular to intermolecular reaction products depends on the relative reactivities of the two different azides, the EM for the intramolecular reaction, and the concentration of the capping agent. Figure 12 shows how the product distribution depends on the concentration of the capping agent. The relative reactivity of the two azides and EM are constants for each substrate, so the ratio of the rates of the intermolecular and intramolecular reactions is expected to be a linear function of the concentration of the capping agent ( $[\text{cap}]$ ). Figure 12 shows that the experimental data fit well to Equation 1, where  $c$  is a constant.

$$A_{\text{inter}}/A_{\text{intra}} = c[\text{cap}] \quad \text{Eq. 1}$$

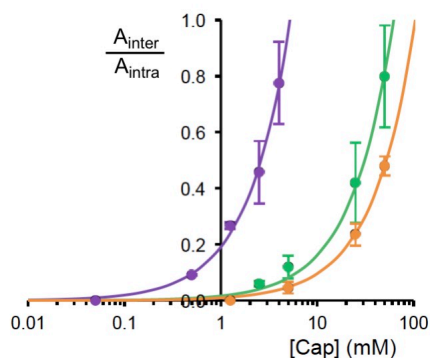


**Figure 12.** Product distribution for the CuAAC reaction of **28** (purple), **27** (green) and **19** (orange) in the presence of different concentrations of capping agent, 4-*t*-butylbenzyl azide ( $[\text{cap}]$ ), plotted as the ratio of the area of the HPLC peaks assigned to the product of the intermolecular reaction with the capping agent ( $A_{\text{inter}}$  for **30**, **35** or **25**) compared with the area of the HPLC peaks assigned to the product of the intramolecular ZIP reaction ( $A_{\text{intra}}$  for **29**, **34** or **24**). Reactions were carried out using **28**, **27** or **19** (25  $\mu\text{M}$ ) and Cu-TBTA (500  $\mu\text{M}$ ) in THF at room temperature. The lines represent the best fit of the data to  $A_{\text{inter}}/A_{\text{intra}} = c[\text{cap}]$ , where  $c$  is a constant related to EM for the intramolecular process.

It is clear that much higher concentrations of the capping agent are required to compete with the antiparallel ZIP reaction. In other words, the EM for formation of the antiparallel duplex is significantly higher than the EM for formation of the parallel duplex. The data in Figure 12 can be used to determine values of EM by extrapolating the curves to the

concentrations of capping agent necessary to obtain a 1:1 ratio of the two products. These concentrations were corrected for the 5-fold difference in reactivity measured for the aromatic and aliphatic azide (see ESI for details) to give the EM values reported in Table 1. The value of EM for the antiparallel ZIP reaction is an order of magnitude higher than EM for the parallel ZIP reaction.

**Table 1. Effective molarities for intramolecular CuAAC reactions measured in THF at room temperature.**

substrate	EM / mM
<b>27</b>	270 $\pm$ 100
<b>28</b>	26 $\pm$ 3
<b>19</b>	530 $\pm$ 100

Pre-ZIP intermediate **19** can form either the parallel or the antiparallel duplex. The results for **27** and **28** suggest that the CuAAC reaction of **19** should lead to the antiparallel duplex as the major product and that the reaction should have the same EM as that determined for **27**. The EM for **19** was therefore determined in the same way by titration with the capping agent. Figure 11(c) compares the reaction pathways for **19** with those for **27** and **28** in the presence of the capping agent. In this case, there are three possible products: intramolecular reaction can give the parallel or antiparallel duplex (*p*-**24** or *a*-**24**) and intermolecular reaction with the capping agent leads to the doubly capped acyclic product **25**. However, the two duplexes cannot be resolved in the LCMS experiment, so only two product peaks, corresponding to the duplex and the doubly capped product, were observed. The product distribution was measured as a function of the concentration of capping agent (orange data in Figure 12), and the results are very similar to those obtained for the substrate that can only form the antiparallel duplex, **27** (green data in Figure 12). The resulting value of EM shown in Table 1 is 530 mM. Comparison with the values of EM for **27** and **28** suggests that the value of EM measured for **19** in this experiment is dominated by formation of the antiparallel duplex. These results suggest that it should be possible to obtain the antiparallel duplex as the major product from the CuAAC reaction of **19**, because the value of EM for formation of the parallel duplex is an order of magnitude lower. However, the  $^1\text{H}$  NMR data shown in Figure 8 indicate that the ratio of

the two product duplexes is 2:1. An investigation of the absolute rates of reaction sheds some light on the origin of this apparent discrepancy.

### Mechanism of the CuAAC reaction

The results above indicate that capping provides an excellent method for controlling the product distribution of template-directed reactions. Provided the capping agent is present in a large excess relative to the substrate (the pre-ZIP intermediate), it is possible to find a concentration of capping agent where the intramolecular ZIP reaction is faster than competing intermolecular reactions with the capping agent, but intermolecular reactions with the capping agent are faster than competing intermolecular reactions between substrates. It should be possible to control the relative rates of the intramolecular ZIP reaction and competing intermolecular reactions between substrates by lowering the concentration of substrate without adding a capping agent. However, the results shown in Figure 6 indicate that this is not the case for the CuAAC reaction used in this system. The literature suggests that the rate-limiting step in the CuAAC reaction is formation of an activated copper species that reacts rapidly with the alkyne to form a copper acetylide complex.<sup>40</sup> This complex then reacts rapidly with the azide to give the triazole product. If the rate of reaction were independent of the concentration of azide, this mechanism could account for the results above. We therefore investigated the effects of concentration on reaction rate.

The CuAAC reaction was carried out on pre-ZIP intermediate **19** in the presence of the capping agent, and the rate of disappearance of the starting material was monitored (Figure 13). Increasing the concentration of **19** by a factor of two had no effect on the half-life of the reaction (compare grey and black data in Figure 13), which suggests that the reaction is first order in substrate. Increasing the concentration of CuTBTA by a factor of two decreased the half-life by a factor of about 3 (compare grey and green data in Figure 13). These results show that both the concentration of substrate and the concentration of copper must appear in the rate equation for the ZIP reaction, so the rate-limiting step is either formation of the copper acetylide complex or reaction of this complex with an azide.

Further insight was obtained by carrying out ZIP reactions on the hetero-dimer template in the absence of capping agent. When the reactions were carried out without any capping agent present, the two pre-ZIP intermediates **27** and **28** gave quite different results. When **27** was subjected to the CuAAC reaction, a single major product was identified in the HPLC chromatogram of the crude reaction mixture. This product has the same molecular weight as the starting material but a different retention time, which suggests that it is the antiparallel duplex **29** (Figure 14(a)). No further reaction of this compound is possible because it has no alkyne groups. In contrast, when **28** was subjected to the CuAAC reaction, two major products were identified in the HPLC chromatogram of the crude reaction mixture. One of the products has the same molecular weight as the starting material but a different retention time, which suggests that it is the parallel duplex **31** (Figure 14(b)). The other product has twice the molecular weight of the starting material, which indicates that it is due to an intermolecular reaction. A possible structure for the intermolecular product **36** is shown in Figure 14(b). Intermolecular reaction is more likely for **28**, because we know that the value of EM for the intramolecular ZIP reaction is an order of magnitude lower than for **27**. However, the rates of formation of the products are not consistent with this explanation. Figure 14(c) compares the rates of formation of **29**, **31** and **36**, when CuAAC reactions were

carried out on **27** and **28** under identical conditions. The rates of formation of all three products are identical. Based on the values of EM, the antiparallel duplex **29** should be formed ten times faster than the parallel duplex **31**, and the intermolecular reaction to give **36** should occur at a quite different rate. The results in Figure 14(c) show that the rate of reaction is independent of the concentration of azide.

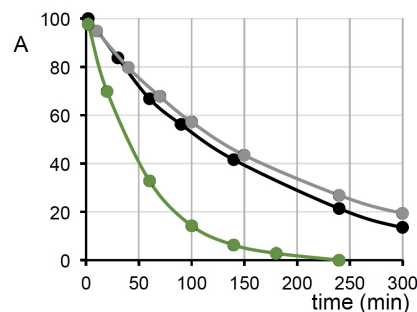


**Figure 13.** Effects of concentration on reaction rate for the CuAAC reaction of **19**. The area of the HPLC peak assigned to the starting material **19** expressed as a percentage of the initial HPLC peak area (A) is plotted as a function of time for reactions carried out using (i) **19** (25 μM) and CuTBTA (50 μM) (black data), (ii) **19** (50 μM) and CuTBTA (50 μM) (grey data) and (iii) **19** (50 μM) and CuTBTA (100 μM) (green data). The lines are drawn as a guide. All reactions were carried out in the presence of 4-*t*-butylbenzyl azide (2.5 mM) in THF at room temperature.

Thus, the overall rate of the CuAAC reaction is determined by rate-limiting formation of the copper acetylide complex, which then reacts rapidly with any available azide. In **27**, there is only one alkyne available to form the copper acetylide complex (Figure 14(a)). This complex could then react intermolecularly to give an oligomeric product or intramolecularly to give **29**. Although the rates of these reactions are both fast and the concentration of azide does not appear in the overall rate law, the concentration of azide does affect the product distribution, because the relative rates of reaction between two different azides depends on the relative concentrations. The concentration of **27** in the reaction mixture is three orders of magnitude lower than the EM for the antiparallel ZIP reaction, so the intramolecular pathway dominates.

In **28**, there are two alkynes, so two different copper acetylide complexes are formed at similar rates. The top reaction channel in Figure 14(b) shows one outcome, which is similar to the reaction pathway shown for **27** in Figure 14(a). The copper acetylide complex could react intermolecularly to give an oligomeric product or intramolecularly to give **31**. The concentration of **28** in the reaction mixture is three orders of magnitude lower than the EM for the parallel ZIP reaction, so the intramolecular pathway dominates. The bottom reaction channel in Figure 14(b) shows the other outcome. In this case, the only available azide is on the same monomer unit as the copper acetylide complex, so an intramolecular reaction is not possible, and the result is an intermolecular reaction. If the copper acetylide complexes could equilibrate rapidly, then the copper could be transferred to the other alkyne, which would then undergo the intramolecular reaction shown in the top reaction channel. The fact that the intermolecular product is formed in similar proportions to the intramolecular product indicates that equilibration of the copper acetylide complexes is slow relative to reaction with azide. In other words, every time an alkyne picks up a copper, it is committed to a very fast reaction with the nearest available azide, and this

mechanism has important consequences for the observed product distributions of the templated reactions.

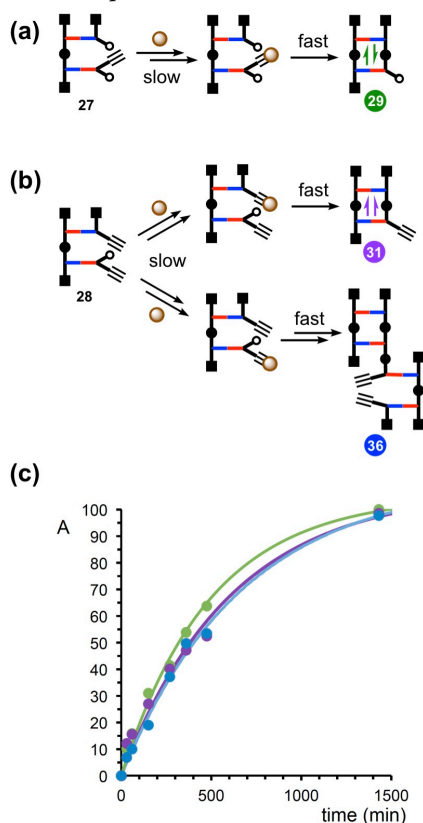


**Figure 14.** Cartoon representation of reaction pathways in the CuAAC reactions of (a) **27** and (b) **28** (brown circles represent an activated copper species). (c) Time dependence of the formation of products **29** (green), **31** (purple) and **36** (blue) in CuAAC reactions of **27** and **28** expressed as a percentage of the final HPLC peak area (A). The lines are drawn as a guide. Reactions were carried out using **27** or **28** (50  $\mu$ M) and CuTBTA (50  $\mu$ M) in THF at room temperature.

#### Controlling the parallel-antiparallel product distribution

These observations have implications for the development of capping strategies to control the product distribution in template-directed synthesis of linear oligomers using CuAAC reactions. Firstly, it is not possible to control reaction rate with concentration, so capping agents provide the only reliable method for controlling the product distribution. Secondly, the mechanism of the CuAAC reaction dictates that the capping agent must be an azide. The use of an alkyne capping agent would interfere with the intramolecular ZIP reaction at all concentrations. Formation of the capping copper acetylide complex and the monomer copper acetylide complexes would occur at similar rates. Once these complexes are formed, fast reaction with an azide will occur, so the capping agent will react indiscriminately with any available azide, and this process will proceed at the same rate as the intramolecular ZIP reaction. Even using stoichiometric amounts of an alkyne capping agent would result in a

mixture of products where the capping agent had reacted with equal probability with each of the azides on the pre-ZIP intermediate.

These insights into the reaction mechanism suggest that it should be possible to change the relative proportions of the parallel and antiparallel duplex formed in the CuAAC reaction by careful choice of the concentration of the capping agent. If no capping agent is used, the CuAAC reaction of **19** should give a 1:1 mixture of the parallel and antiparallel product duplexes, because the two alkynes in the pre-ZIP intermediate will react with the activated copper species at similar rates. The resulting copper acetylide complexes could react intermolecularly to give an oligomeric product or intramolecularly to give a duplex. The values of EM for the parallel and antiparallel ZIP reactions are both orders of magnitude higher than the concentration of **19** used in the CuAAC reactions, so the intramolecular pathway will dominate in both cases. In other words, the product distribution is determined by the relative amounts of different alkynes available for reaction with the activated copper species. However, addition of the capping agent clearly affects this product distribution, because Figure 8 shows that the amount of antiparallel duplex formed is twice the amount of parallel duplex in the presence of 1.25 mM capping agent.

Figure 15 illustrates possible reaction pathways in the presence of a capping agent. There is a bifurcation in the first step, because the two copper acetylide complexes are formed at the same rate. There is a second bifurcation in the second reaction step, because each of these complexes can react intermolecularly with the capping agent or intramolecularly to give a duplex. The relative rates of these processes are determined by the relative concentrations of the intramolecular and capping azides. The EM for the antiparallel ZIP reaction is an order of magnitude higher than for the parallel ZIP reaction, so as the concentration of capping azide is increased, the capping agent is more likely to intercept the copper acetylide complex that leads to the parallel duplex (bottom reaction channel in Figure 15) than the copper acetylide complex that leads to the antiparallel duplex (top reaction channel). If the values of EM for the two intramolecular processes are sufficiently separated, it should be possible to find a concentration of capping agent, which is higher than the EM for the parallel ZIP reaction and lower than the EM for the antiparallel ZIP reaction. The consequences are illustrated in Figure 15. In the second bifurcation step in the top reaction channel, intramolecular reaction to form the antiparallel duplex is faster than reaction with the capping agent, and the product of this reaction is subsequently capped to give **a-24**. In the bottom reaction channel, reaction with the capping agent is faster than the intramolecular reaction to form the parallel duplex. When the product of this reaction reacts with a second activated copper species, the resulting copper acetylide complex can react intramolecularly to give the antiparallel duplex or intermolecularly to give the doubly capped product. In this case the intramolecular is faster, so the antiparallel duplex is formed again. Figure 15 shows that it does not matter which of the two alkynes reacts with the activated copper species first, because both reaction channels lead to the same capped antiparallel duplex.

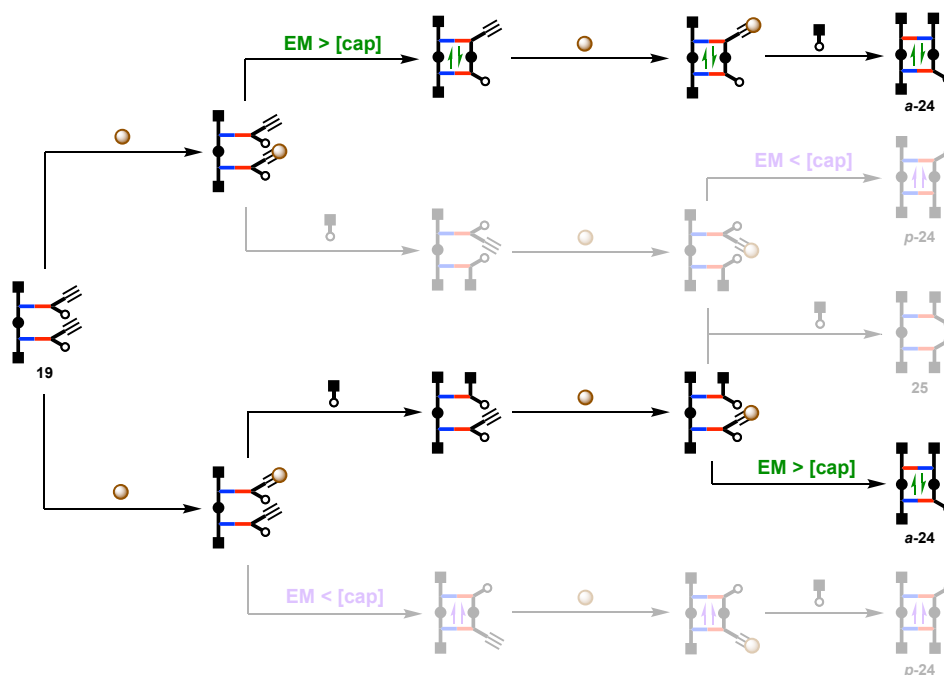


**Figure 15.** Cartoon representation of the different reaction pathways possible for the CuAAC reaction of **19** in the presence of a capping agent. In the first step, the activated copper species (brown circles) can react with either of the two alkynes in **19**. The resulting copper acetylide complexes can undergo intermolecular reactions with the capping agent or intramolecular reactions to give duplexes at rates determined by the relevant EM and the concentration of capping agent [cap]. The outcome is illustrated for conditions where [cap] is greater than EM for the parallel ZIP reaction (purple) and less than EM for the antiparallel ZIP reaction (green). Less likely reaction channels are greyed out. The two most probable reaction pathways both lead to the capped antiparallel duplex, **a-24**.

Figure 16 shows  $^1\text{H}$  NMR spectra of the products obtained by carrying out the CuAAC reaction on **19** in the presence of increasing amounts of capping agent. The two sets of signals in the triazole region of the spectra were assigned as the antiparallel duplex **a-24** (green) and parallel duplex **p-24** (purple) based on the values of EM in Table 1. As the concentration of capping agent was increased, the amount of parallel duplex formed decreased. At a concentration of 5 mM capping agent, the antiparallel duplex was the only product detected. As shown in Figure 10, the amount of doubly capped product is also negligible at this concentration, so under these conditions, 5 mM azide capping agent provides excellent control over the product distribution of the CuAAC reaction by blocking intermolecular oligomerisation reactions and the parallel ZIP reaction. These results should be transferrable to longer oligomers. Alkynes in the middle of a chain will always have a choice between parallel and antiparallel ZIP reactions and will preferentially form antiparallel linkages. There is only one alkyne for which the antiparallel ZIP reaction is not an option, one of the terminal alkynes, but when the capping agent is present at a concentration of 5 mM, it will preferentially react with this group preventing the formation a parallel linkage.

The duplex product **a-24** obtained from the ZIP reaction of **19** in the presence of the capping azide was hydrolysed using lithium hydroxide. Cleavage of the duplex was quantitative giving the starting benzoic acid homo-dimer template and the templated phenol homo-dimer copy as the only products (see ESI).

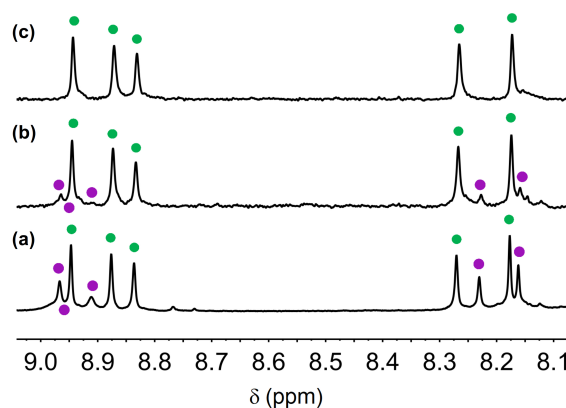


**Figure 16.** Partial 500 MHz  $^1\text{H}$ -NMR spectra in  $\text{DMSO}-d_6$  at 298 K of the duplex products obtained from CuAAC reactions of **19** in the presence of different concentrations of capping agent (4-*t*-butylbenzyl azide): (a) 1.25 mM, (b) 2.5 mM, (c) 5 mM. All reactions were carried out using **19** (25  $\mu\text{M}$ ) and CuTBTA (50-500  $\mu\text{M}$ ) in THF at room temperature. The triazole signals are labelled green for **a-24** and purple for **p-24**.

## Conclusions

Template-directed synthesis is the method used in biology for the synthesis of linear oligomers of defined sequence. Although templating strategies are commonly used in supramolecular chemistry for the synthesis of macrocyclic oligomers, methods for the template-directed synthesis of linear oligomers are still in their infancy. Linear oligomers present a challenge for current templating methodologies,

because the chain ends represent reactive sites that can lead to macrocyclization or further intermolecular oligomerisation. We show here that covalent template-directed oligomerisation reactions in combination with capping agents that block further reaction on the chain ends provides a promising solution to the controlled synthesis of linear oligomers. By using kinetically inert covalent bonds to attach the monomer units to the template, it is possible to operate at very high dilution without compromising the template-monomer interactions. Intramolecular templated reactions are much more favourable than intermolecular reactions at high dilution, which allows the use of an excess of a capping agent to terminate the oligomer chains without competing with the desired monomer-monomer coupling reactions.

The covalent bond used to attach the monomer units to the template is an ester between a phenol and a benzoic acid. The phenol and benzoic acid monomer building blocks were each equipped with an alkyne and an azide so that they could be oligomerised using CuAAC reactions. Covalent template-directed oligomerisation reactions were carried out on two different dimeric templates in the presence of an azide capping agent. In the absence of the capping agent, complex product mixtures were obtained due to intermolecular reactions. It was not possible to reduce these side reactions by dilution, because the rate limiting step of the CuAAC reaction is formation of an activated copper complex, and the resulting copper acetylide reacts rapidly with the nearest available azide. However, it was possible to find a concentration of capping agent that blocked the undesired intermolecular reaction without interfering with the desired intramolecular reaction, resulting in a quantitative yield of the templated dimeric product.

The backbone resulting from the CuAAC reaction in this system has a direction, which means that the reaction on the template gives two isomeric products, which have parallel and antiparallel backbones. Titration of the capping agent allowed determination of the effective molarities for these two templated reactions, and the reaction leading to the antiparallel duplex is significantly faster than the reaction leading to the parallel duplex. Thus it was possible to find a concentration of capping agent that gives exclusively the antiparallel dimer product.

The findings are not limited to the specific backbone architecture described here. Any orthogonal combination of base-pairing and backbone chemistry could be used, provided the resulting bonds are kinetically inert, and the capping strategy provides a general method for controlling the product distribution in template-directed synthesis of linear oligomers. It is likely that capping will be more effective in controlling covalent template-directed oligomerisation reactions compared with non-covalent templating, because it is possible to operate at lower dilutions. Importantly for CuAAC reactions, the mechanism dictates that the capping agent must be an azide and cannot be an alkyne.

### Supporting Information

Materials and methods, synthetic procedures and compound characterization, and details of LCMS methods used for reaction monitoring are available in the Supplementary Materials. This material is available free of charge via the Internet at <http://pubs.acs.org>.

### AUTHOR INFORMATION

#### Corresponding Author

\* Department of Chemistry, University of Cambridge, Lensfield Road, Cambridge CB2 1EW, UK.

E-mail: [herchelsmith.orgchem@ch.cam.ac.uk](mailto:herchelsmith.orgchem@ch.cam.ac.uk)

### Funding Sources

European Research Council (ERC-2012-AdG 320539-duplex) and the Herchel Smith Fund for funding.

### ACKNOWLEDGMENT

We thank the ERC (ERC-2012-AdG 320539-duplex) and the Herchel Smith Fund for funding.

### REFERENCES

- (1) *Templated Organic Synthesis*; Diederich, F.; Stang, P. J., Eds.; Wiley-VCH: New York, 2000.
- (2) Lo, P. K.; Sleiman, H. F. Nucleobase-Templated Polymerization: Copying the Chain Length and Polydispersity of Living Polymers into Conjugated Polymers. *J. Am. Chem. Soc.* **2009**, *131*, 4182-4183.
- (3) Ayme, J.-F.; Beves, J. E.; Campbell, C. J.; Leigh, D. A. Template synthesis of molecular knots. *Chem. Soc. Rev.* **2013**, *42*, 1700-1712.
- (4) Lewis, J. E. M.; Beer, P. D.; Loeb, S. J.; Goldup, S. M. Metal ions in the synthesis of interlocked molecules and materials. *Chem. Soc. Rev.* **2017**, *46*, 2577-2591.
- (5) Chen, Z.; Liu, D. R. Nucleic Acid-Templated Synthesis of Sequence-Defined Synthetic Polymers. In *Sequence-Controlled Polymers*; J.-F. Lutz, Ed., Wiley-VCH Verlag GmbH & Co. KGaA, 2018; pp.49-90.
- (6) O'Reilly, R. K.; Turberfield, A. J.; Wilks, T. R. The Evolution of DNA-Templated Synthesis as a Tool for Materials Discovery. *Acc. Chem. Res.* **2017**, *50*, 2496-2509.
- (7) O'Flaherty, D. K.; Kamat, N. P.; Mirza, F. N.; Li, L.; Prywes, N.; Szostak J. W. Copying of Mixed-Sequence RNA Templates inside Model Protoplasts. *J. Am. Chem. Soc.* **2018**, *140*, 5171-5178.
- (8) Inthasot, A.; Tung, S.-T.; Chiu, S.-H. Using Alkali Metal Ions To Template the Synthesis of Interlocked Molecules. *Acc. Chem. Res.* **2018**, *51*, 1324-1337.
- (9) Bols, P. S.; Anderson, H. L. Template-Directed Synthesis of Molecular Nanorings and Cages. *Acc. Chem. Res.* **2018**, *51*, 2083-2092.
- (10) Pedersen, C. J. Cyclic polyethers and their complexes with metal salts. *J. Am. Chem. Soc.* **1967**, *89*, 7017-7036.
- (11) McMurry, T. J.; Raymond, K. N.; Smith, P. H. Molecular recognition and metal ion template synthesis. *Science* **1989**, *244*, 938-943.
- (12) Berrocal, J. A.; Cacciapaglia, R.; Di Stefano, S.; Mandolini, L. Target-induced amplification in a dynamic library of macrocycles. A quantitative study. *New J. Chem.* **2012**, *36*, 40-43.
- (13) Kamonsutthipajit, N.; Anderson, H. L. Template-directed synthesis of linear porphyrin oligomers: classical, Vernier and mutual Vernier. *Chem. Sci.* **2017**, *8*, 2729-2740.
- (14) Schill, G.; Lüttringhaus, A. The Preparation of Catena Compounds by Directed Synthesis. *Angew. Chem. Int. Ed.* **1964**, *3*, 546-547.
- (15) Moneta, W.; Baret, P.; Pierre, J.-L. Design and syntheses of macrocyclic hosts containing convergent hydroxy groups. *J. Chem. Soc., Chem. Commun.* **1985**, 899-901.
- (16) Zimmerman, S. C.; Wendland, M. S.; Rakow, N. A.; Zharov, I.; Suslick, K. S. Synthetic hosts by monomolecular imprinting inside dendrimers. *Nature* **2002**, *418*, 399-403.
- (17) Zimmerman, S. C.; Zharov, I.; Wendland, M. S.; Rakow, N. A.; Suslick, K. S. Molecular Imprinting Inside Dendrimers. *J. Am. Chem. Soc.* **2003**, *125*, 13504-13518.
- (18) Hiratani, K.; Kaneyama, M.; Nagawa, Y.; Koyama, E.; Kanesato, M. Synthesis of [1]Rotaxane via Covalent Bond Formation and Its Unique Fluorescent Response by Energy Transfer in the Presence of Lithium Ion. *J. Am. Chem. Soc.* **2004**, *126*, 13568-13569.
- (19) Kawai, H.; Umehara, T.; Fujiwara, K.; Tsuji, T.; Suzuki, T. Dynamic covalently bonded rotaxanes cross-linked by imine bonds between the axle and ring: inverse temperature dependence of subunit mobility. *Angew. Chem. Int. Ed.* **2006**, *45*, 4281-4286.
- (20) Lin, N.-T.; Lin, S.-Y.; Lee, S.-L.; Chen, C.-h.; Hsu, C.-H.; Hwang, L.-P.; Xie, Z.-Y.; Chen, C.-H.; Huang, S.-L.; Luh, T.-Y. From polynorbornene

to the complementary polynorbornene by replication. *Angew. Chem. Int. Ed.* **2007**, *46*, 4481–4485.

(21) Schweez, C.; Shushkov, P.; Grimme, S.; Höger, S. Synthesis and Dynamics of Nanosized Phenylene-Ethynylene-Butadiynylene Rotaxanes and the Role of Shape Persistence. *Angew. Chem. Int. Ed.* **2016**, *55*, 3328–3333.

(22) Steemers, L.; Wanner, M. J.; Lutz, M.; Hiemstra, H.; Van Maarseveen, J. H. Synthesis of spiro quasi[1]catenanes and quasi[1]rotaxanes via a templated backfolding strategy. *Nat. Commun.* **2017**, *8*, 15392.

(23) Anderson, S.; Anderson, H. L. Templates in Organic Synthesis: Definitions and Roles. In *Templated Organic Synthesis*; Diederich, F.; Stang, P. J., Eds.; Wiley-VCH: New York, 2000; pp 1–38.

(24) Joyce, C. M.; Benkovic, S. J. DNA polymerase fidelity: kinetics, structure, and checkpoints. *Biochemistry* **2004**, *43*, 14317–14324.

(25) Berdis, A. J. Mechanisms of DNA polymerases. *Chem. Rev.* **2009**, *109*, 2862–2879.

(26) Nudler, E. *Ann. RNA polymerase active center: the molecular engine of transcription. Rev. Biochem.* **2009**, *78*, 335–361.

(27) Núñez-Villanueva, D.; Ciaccia, M.; Iadevaia, G.; Sanna, E.; Hunter, C. A. Sequence information transfer using covalent template-directed synthesis. *doi: 10.1039/C9SC01460H*.

(28) Ellington, A. D.; Szostak, J. W. In vitro selection of RNA molecules that bind specific ligands. *Nature* **1990**, *346*, 818–822.

(29) Chen, K.; Arnold, F. H. Tuning the activity of an enzyme for unusual environments: sequential random mutagenesis of subtilisin E for catalysis in dimethylformamide. *Proc Natl Acad Sci U.S.A.* **1993**, *90*, 5618–5622.

(30) Meldal, M.; Tornøe, C. W. Cu-Catalyzed Azide–Alkyne Cycloaddition. *Chem. Rev.* **2008**, *108*, 2952–3015.

(31) Hein, J. E.; Fokin, V. V. Copper-catalyzed azide–alkyne cycloaddition (CuAAC) and beyond: new reactivity of copper(I) acetylides. *Chem. Soc. Rev.* **2010**, *39*, 1302–1315.

(32) Kukwikila, M.; Gale, N.; El-Sagheer, A. H.; Brown, T.; Tavassoli, A. Assembly of a biocompatible triazole-linked gene by one-pot click-DNA ligation. *Nat. Chem.* **2017**, *9*, 1089–1098.

(33) Sawamoto, M.; Furukawa, A.; Higashimura, T. End-capping analysis of cationic polymerization of styrene derivatives with sodium  $\beta$ -naphthoxide as capping agent. 1. Concentration and chain-length distribution of the propagating species in styrene polymerization. *Macromolecules* **1983**, *16*, 518–522.

(34) Ando, T.; Kamigaito, M.; Sawamoto, M. Silyl Enol Ethers: End-Capping Agents for Living Radical Polymerization of Methyl Methacrylate with Ruthenium Complex. *Macromolecules* **1998**, *31*, 6708–6711.

(35) Braunecker, W. A.; Matyjaszewski, K. Controlled/living radical polymerization: Features, developments, and perspectives. *Prog. Polym. Sci.* **2007**, *32*, 93–146.

(36) Aoshima, S.; Kanaoka, S. A Renaissance in Living Cationic Polymerization. *Chem. Rev.* **2009**, *109*, 5245–5287.

(37) Harris, J. D.; Carter, K. R. A one-pot strategy to improve end-capping efficacy in Stille poly-condensations. *Polym. Chem.* **2018**, *9*, 1132–1138.

(38) Li, W.; Tian, T.; Zhu, W.; Cui, J.; Ju, Y.; Li, G. Metal-free click approach for facile production of main chain poly(bile acid)s. *Polym. Chem.* **2013**, *4*, 3057–3068.

(39) Kirby, A. Effective Molarities for Intramolecular Reactions. *J. Adv. Phys. Org. Chem.* **1980**, *17*, 183–278.

(40) Rodionov, V. O.; Fokin, V. V.; Finn, M. G. Mechanism of the ligand-free CuI-catalyzed azide–alkyne cycloaddition reaction. *Angew. Chem. Int. Ed.* **2005**, *44*, 2210–2215.

